1521-009X/49/2/152–158$35.00
DRUG METABOLISM AND DISPOSITION
https://doi.org/10.1124/dmd.120.000136
Drug Metab Dispos 49:152–158, February 2021

Impact of Direction of Transport on the Evaluation of Inhibition Potencies of Multidrug and Toxin Extrusion Protein 1 Inhibitors

Asami Saito, Naoki Ishiguro, Masahito Takatani, Bojan Bister, and Hiroyuki Kusuhara

Pharmacokinetics and Non-Clinical Safety Department, Nippon Boehringer Ingelheim Co., Ltd., Kobe, Japan (A.S., N.I, M.T., B.B.) and Laboratory of Molecular Pharmaceutics, Graduate School of Pharmaceutical Sciences, The University of Tokyo, Tokyo, Japan (H.K.)

Received June 8, 2020; accepted November 23, 2020

ABSTRACT

Multidrug and toxin extrusion (MATE) transporters are expressed on the luminal membrane of renal proximal tubule cells and extrude their substrates into the luminal side of the tubules. Inhibition of MATE1 can reduce renal secretory clearance of its substrate drugs and lead to drug-drug interactions (DDIs). To address whether IC_{50} values of MATE1 inhibitors with regard to their extracellular concentrations are affected by the direction of MATE1-mediated transport, we established an efflux assay of 1-methyl-4-phenylpyridinium (MPP^+) and metformin using the human embryonic kidney 293 model transiently expressing human MATE1. The efflux rate was defined by reduction of the cellular amount of MPP^+ and metformin for 0.25 minutes shortly after the removal of extracellular MPP^+ and metformin. Inhibition potencies of 12 inhibitors toward MATE1-mediated transport were determined in both uptake and efflux assays. When MPP^+ was used as a substrate, 8 out of 12 inhibitors showed comparable IC_{50} values between assays (<4-fold). IC_{50} values from the efflux assays were higher for cimetidine (9.9-fold), trimethoprim (10-fold), famotidine (6.4-fold), and cephalexin (>3.8-fold). When metformin was used as a substrate, IC_{50} values of the tested inhibitors when evaluated using uptake and efflux assays were within 4-fold of each other, with the exception of cephalexin (>4.7-fold). IC_{50} values obtained from the uptake assay using metformin showed smaller IC_{50} values than those from the efflux assay. Therefore, the uptake assay is recommended to determine IC_{50} values for the DDI predictions.

SIGNIFICANCE STATEMENT

In this study, a new method to evaluate IC_{50} values of extracellular added inhibitors utilizing an efflux assay was established. IC_{50} values were not largely different between uptake and efflux directions but were smaller for uptake. This study supports the rationale for a commonly accepted uptake assay with metformin as an in vitro probe substrate for multidrug and toxin extrusion 1–mediated drug-drug interaction risk assessment in drug development.

Introduction

The multidrug and toxic compound extrusion (MATE) family of transporters is ubiquitously expressed in organisms from several kingdoms of life, including archaea, bacteria, and plants, and exports cationic compounds using the H^+ or Na^+ gradient across plasma membranes. The human MATE orthologs MATE1 (SLC47A1) and MATE2-K (SLC47A2) are expressed on the brush-border membrane of proximal tubule cells and work as organic cations/H^+ antiporters driven by an H^+ gradient (Yonezawa and Inui, 2011a; Motohashi and Inui, 2013). Although 1-methyl-4-phenylpyridinium (MPP^+) and metformin are prototypical substrates of MATEs, extensive studies have identified various compounds as MATE1 and MATE2-K substrates, including endogenous metabolites such as creatinine (Terada and Inui, 2008). Quantitative targeted proteomics revealed abundant MATE1 expression in the human kidney cortex, whereas MATE2-K expression was detectable but below the lower limit of quantification (Prasad et al., 2016), suggesting that MATE1 is the major MATE isoform in the kidney. MATEs also play an important role in several clinical drug-drug interactions (DDIs) (Tsuda et al., 2009; Kusuhara et al., 2011; Ito et al., 2012), renal toxicities (Yonezawa and Inui, 2011b; Li et al., 2013), and drug efficacy (Becker et al., 2009; Stocker et al., 2013). MATE-mediated DDIs can result in a reduction in the renal clearance of coadministered drugs, or other compounds, that are MATE substrates (Ivanyuk et al., 2017). A reversible increase in levels of serum creatinine, a frequently used biomarker for kidney function, can occur by inhibiting its MATE-mediated tubular secretion (Chu et al., 2016; Nakada et al., 2019). Because of the emerging importance of MATE transporters in DDIs, regulatory authorities recently revised their guidelines for drug interaction studies to include MATEs. As such, sponsors now routinely evaluate the in vitro DDI potential of investigational compounds toward these transporters (European Medicines Agency, 2012; Ministry of Health, Labor and Welfare, 2018; U.S. Food and Drug Administration, 2020).

To profile compounds that interact with MATE transporters, the uptake of in vitro probe substrates into cells that overexpress a MATE transporter, defined in this paper as an "uptake assay" or "uptake direction," is one of the most commonly used methods. This methodology assumes that MATEs exhibit symmetric transport in both uptake and efflux directions. Considering the physiologic role of MATEs as efflux transporters in the kidney, there are concerns about the impact of the direction of transport on estimation of IC_{50} values. Several crystal

This study was supported by Nippon Boehringer Ingelheim Co., Ltd.
https://doi.org/10.1124/dmd.120.000136.
This article has supplemental material available at dmd.aspetjournals.org.

ABBREVIATIONS: AUC, area under the curve; DDI, drug-drug interaction; HEK293, human embryonic kidney 293; $I_{max,u}$, maximum unbound inhibitor concentration; MATE, multidrug and toxin extrusion; MPP^+, 1-methyl-4-phenylpyridinium; SLC, solute carrier family.

structures of MATE orthologs have been reported (NorM-VC from *Vibrio cholerae*, DinF-BH from *Bacillus halodurans*, pfMATE from *Pyrococcus furiosus*, and eMATE from *Arabidopsis thaliana*) (He et al., 2010; Lu et al., 2013; Tanaka et al., 2013; Miyauchi et al., 2017); however, most of the available structures to date only focus on outward-facing portions of the protein, and therefore symmetry of MATE transporters across cell membranes is not well understood. Whereas Dangprapai and Wright (2011) revealed that the inward- and outward-facing MATE1 protein is symmetric by checking the kinetic interaction of H^+ with MATE1, no information regarding symmetric interaction substances other than H^+ is available.

In this study, we developed the efflux assay to simply focus on the impact of the direction of transport toward IC_{50} determination and compared the inhibition potency of 12 known MATE transporter inhibitors with regard to their extracellular concentrations for both uptake and efflux of two MATE1 substrates, MPP^+ and metformin, in MATE1-overexpressing cells. Furthermore, DDI predictions involving MATE1 were assessed using the $I_{max,u}/IC_{50}$ approach as currently recommended by regulatory agencies.

Materials and Methods

Chemicals and Reagents. Unlabeled metformin was purchased from Wako Pure Chemical Industries (Osaka, Japan), and unlabeled MPP^+ was purchased from Sigma-Aldrich (St. Louis, MO). [^{14}C]Metformin (100 mCi/mmol) and [^{3}H]metformin (8 Ci/mmol) were purchased from Moravek Biochemicals (Brea, CA), and [^{3}H]MPP^+ (80 Ci/mmol) was purchased from American Radiolabeled Chemicals (Saint Louis, MO). All other chemicals and reagents were of analytical grade and are commercially available.

Cell Culture and Transfection. HEK293 cells transiently expressing human MATE1 were cultured in poly(D-lysine)–coated 24-well plates as described in our previous study (Lechner et al., 2016). Culture medium supplemented with 5 mM sodium butyrate was added approximately 24 hours after transfection to induce transporter gene expression. Uptake and efflux experiments were conducted approximately 48 hours after transfection.

Uptake Experiments Using Transiently Transfected HEK293 Cells. Cells were washed twice and incubated with transport buffer supplemented with 20 mM NH_4Cl for 10 minutes at 37°C. The medium was replaced with NH_4Cl-free transport buffer, and cells were incubated for an additional 5 minutes for intracellular preacidification. The composition of transport buffer was as follows: 130 mM KCl, 2 mM KH_2PO_4, 1.2 mM $MgSO_4$, 1 mM $CaCl_2$, 20 mM HEPES, and 5 mM glucose. Uptake was initiated by replacing buffer with transport buffer containing radiolabeled [^{3}H]MPP^+ or [^{14}C]metformin with or without inhibitors. Uptake was terminated at the designated incubation times by removal of drug solution followed by an addition of ice-cold transport buffer. The cells were then washed three times with 0.5 ml of ice-cold transport buffer. Cells were solubilized with NaOH for 1 hour at 37°C, and the lysate was neutralized by adding HCl. Aliquots of the cell lysates were transferred to scintillation vials containing scintillation cocktail (Ultima Gold XR; PerkinElmer, Waltham, MA), and radioactivity was measured in a liquid scintillation counter (TRI-CARB 3110TR; PerkinElmer). The protein concentration was determined using the Lowry method with bovine serum albumin as the protein standard (Lowry et al., 1951).

Efflux Experiments Using Transiently Transfected HEK293 Cells. Cells were washed twice and incubated with NH_4Cl-free transport buffer for 30 minutes at 37°C. Then, medium was replaced with NH_4Cl-free transport buffer containing [^{3}H]MPP^+ or [^{3}H]metformin and incubated for an additional 10 minutes to preload the labeled substrate into the cells. Efflux was initiated by replacing preloading buffer with transport buffer supplemented with 20 mM NH_4Cl with and without inhibitors. Termination of efflux, cell lysis, radioactivity measurement, and determination of protein concentration were done as described in uptake experiments (Supplemental Fig. 3). Total intracellular substrate concentration was determined assuming 6.5 μl as cellular volume per milligram protein (Gillen and Forbush, 1999).

Determination of Intracellular pH. Intracellular pH was determined using a pH-sensitive fluorescent dye. HEK293 cells expressing MATE1 were preloaded with 2′,7′-bis-(2-carboxyethyl)-5-(and-6)-carboxyfluorescein acetoxymethyl at 37°C for 30 minutes. The fluorescence intensity (excitation at 488 and 460 nm, emission at 535 nm) was measured, and the ratio of fluorescence from the two wavelengths was monitored in a fluorescence plate reader (Enspire; PerkinElmer). Intracellular pH of MATE1-HEK293 cells was calibrated using standardized pH buffers containing 10 μM nigericin (Thomas et al., 1979).

Data Analysis. MATE1-mediated uptake clearance was calculated by normalizing the amount of radioactivity inside the cells to that in the buffer and the protein concentration in each well using the following equation:

$$Uptake\ CL = \frac{X_{cell}}{C_{buffer}},$$

where *Uptake CL* is the uptake clearance (microliters per designated time point per milligram), X_{cell} is the radioactivity in the cells (dpm per designated time per well), and C_{buffer} is the concentration of radioactivity in the buffer (dpm per microliter). Uptake CL was normalized by the amount of total cellular protein (milligrams per well). MATE1-mediated uptake was calculated by subtracting the uptake into mock vector-transfected cells from that into MATE1-transfected cells.

MATE1-mediated efflux clearance was calculated by subtracting the remaining amount of substrate within the cells from that in the presence of 100 μM pyrimethamine, which was assumed to inhibit MATE1 completely, and was normalized by area under the curve (AUC) of intracellular substrate concentration-time curve and protein concentration in each well using the following equation:

$$Efflux\ CL = \frac{X_{t_n,pyr} - X_{t_n}}{AUC_{0-t_n}},$$

where *Efflux CL* is the efflux clearance (microliters per designated time per milligram), $X_{t_n,pyr}$ is the radioactivity remaining in the cells at t_n in the presence of 100 μM pyrimethamine (dpm per designated time per well), X_{t_n} is the radioactivity remained in the cells at t_n (dpm per designated time per well), and *Efflux CL* was normalized by the amount of protein (milligrams per well).

Because the uptake of probe substrates during the preloading phase is largely different, and it is difficult to use the identical initial intracellular concentration between MATE1-transfected cells and mock vector-transfected cells, MATE1-transfected cells incubated in presence of 100 μM pyrimethamine were used as control cells assuming no MATE1 activity.

Decrease of the total intracellular substrate concentration during efflux incubations was assumed to follow first-order elimination, and the change of intracellular concentration over time was described by

$$AUC_{0-t_n} = \frac{t_n \times (C_0 - C_{t_n})}{\ln(C_0/C_{t_n})},$$

where *AUC* is area under the total intracellular substrate concentration-time curve (micromolar × minute), t_n is efflux incubation time (minutes), C_0 is the initial total intracellular substrate concentration (micromolar), and C_{t_n} (micromolar) is the total intracellular substrate concentration at t_n. t_n was set to 0.25 minutes as the minimum feasible time.

The IC_{50} of each inhibitor was determined using GraphPad PRISM software version 8.3.0 (GraphPad Software, San Diego, CA) based on the four-parameter logistic equation

$$CL = CL_{min} + \left(\frac{(CL_{max} - CL_{min})}{1 + 10^{((logIC_{50} - I) \times Hill)}}\right),$$

where *CL* represents the uptake or efflux clearance, *I* is the concentration of inhibitor in the extracellular buffers, and *Hill* is the slope factor.

Results

Effect of NH_4Cl on Intracellular pH to Modulate the H^+ Gradient. Acute exposure to NH_4Cl increased intracellular pH apparently to around pH 8.0 at all NH_4Cl concentrations (a pH greater than 8 could not be reliably determined because of a limitation of the method, Supplemental Fig. 1). At 20 mM NH_4Cl, the intracellular pH was greater than 8.0 immediately after the medium change. It was

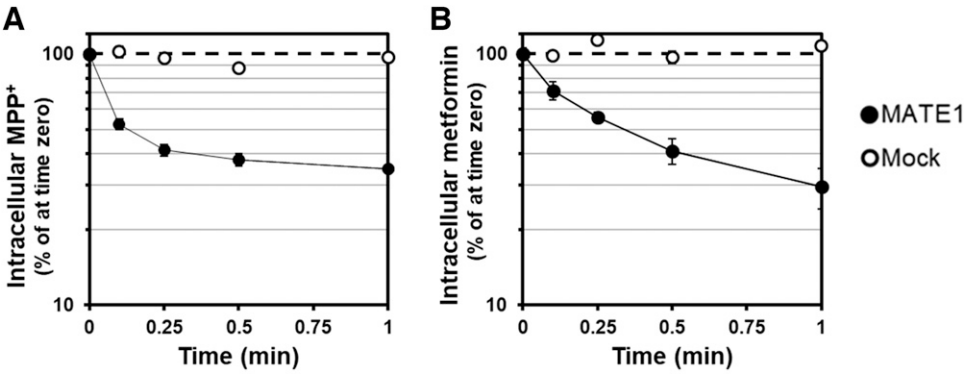

Fig. 1. Time profiles of intracellular [^{3}H]MPP$^+$ (A) and [^{3}H]metformin (B) in MATE1-expressing HEK293 cells. After preloading [^{3}H]MPP$^+$ (0.01 μM) and [^{3}H]metformin (0.1 μM) for 10 minutes, efflux was initiated in 20 mM NH_4Cl buffer at pH 7.4, and the remaining concentrations of substrates in the cells were measured. Each point represents the mean value ± S.D. (n = 3).

maintained up to 10 minutes after the medium change and then gradually returned to basal pH (Supplemental Fig. 2).

Washout of NH_4Cl by replacement with buffer lacking NH_4Cl decreased intracellular pH in a concentration-dependent manner. In our previous study, in which 20 mM NH_4Cl was used for intracellular preacidification (Lechner et al., 2016), the intracellular pH in the uptake assay was around 6.5 and was maintained for several minutes, which is a sufficient duration, as the incubation time was 1 minute. Subsequently, 20 mM NH_4Cl was used in all experiments to generate an artificial pH gradient.

Time and Concentration-Dependent Efflux of [^{3}H]MPP$^+$ and [^{3}H]Metformin. MPP$^+$ and metformin were selected as probe substrates in this study because they are the most-studied prototypical and/or clinically relevant organic cations for MATE assays. In addition, IC_{50} values toward MATE1 using these two substrates were comparable in uptake assays in previous studies (Lechner *et al.*, 2016; Martínez-Guerrero *et al.*, 2016b).

The efflux of MPP$^+$ and metformin from MATE1-expressing cells or mock vector-transfected cells is shown in Fig. 1. A time-dependent decrease of intracellular substrate concentration was only observed in MATE1-expressing cells but not in control cells. The decrease of intracellular substrates was curve-linear in semi-log plots. In particular, this tendency was remarkable when MPP$^+$ was used (Fig. 1). According to the preliminary experiment, it was not practical to determine IC_{50} values in incubation times shorter than 0.25 minutes because of the small change in the cellular amount of MPP$^+$ or metformin, resulting in a non-negligible experimental variability of the efflux rates. The subsequent analysis was conducted at 0.25 minutes as the minimum feasible incubation time in further assays for both probe substrates.

Efflux clearance of MPP$^+$ and metformin from MATE1-expressing cells decreased as shown by an increase of intracellular concentration of substrates (Supplemental Fig. 4), resulting in apparent K_m values of 10–100 μM (MPP$^+$) and 100–1000 μM (metformin), respectively. The nominal concentrations of MPP$^+$ and metformin in preloading solutions were set at 0.05 and 0.75 μM, respectively, because the experimentally determined total intracellular concentrations of the substrates used were 1 and 10 μM, which is similar to the substrate concentrations used in the inhibition study in the uptake direction (Lechner et al., 2016).

Comparison of Uptake and Efflux IC_{50} Using MPP$^+$ and Metformin as a Substrate. Inhibition potencies of dolutegravir, vandetanib, cephalexin, ranolazine, lansoprazole, and cobicistat, which are reported to cause clinical DDIs via inhibition of MATE1, were investigated in the uptake direction (Supplemental Fig. 5; Table 1), along with the six compounds investigated previously (Lechner et al., 2016). Additionally, inhibition potencies of these 12 compounds were determined in the efflux direction. In both assays, IC_{50} values were defined by inhibitor concentrations in the buffer added to the outside of the cells (Figs. 2–4; Supplemental Fig. 5; Table 1).

TABLE 1

DDI risk assessment based on IC_{50} values from uptake/efflux directions and plasma unbound C_{max}

IC_{50} values were estimated by nonlinear regression analysis and are given as means ± S.D.

Inhibitor	IC_{50}, MATE1				$C_{max,u}$	Metformin AUC Change	$C_{max,u}/IC_{50,\ Metfromin}$	
	MPP$^+$		Metformin					
	Uptake	Efflux	Uptake	Efflux			Uptake	Efflux
	μM					%		
Pyrimethamine*	0.492 ± 0.039	1.19 ± 0.061	0.313 ± 0.052	0.502 ± 0.058	0.298	35.3–170	0.95	0.59
Cimetidine*	4.43 ± 0.05	43.8 ± 0.13	2.56 ± 0.04	6.12 ± 0.077	7.74	46.2–54.2	3.0	1.3
Trimethoprim*	8.16 ± 0.06	84.5 ± 0.087	4.13 ± 0.09	11.3 ± 0.13	8.88	21.5–68.6	2.2	0.79
Quinidine*	6.77 ± 0.08	15.5 ± 0.094	5.82 ± 0.06	5.00 ± 0.12	1.34	No data	0.23	0.27
Ondansetron*	0.797 ± 0.025	0.935 ± 0.15	0.436 ± 0.083	0.624 ± 0.19	0.0471	21	0.11	0.076
Famotidine*	1.670 ± 0.03	10.7 ± 0.12	0.905 ± 0.046	3.11 ± 0.12	1	2.7	1.1	0.32
Dolutegravir	7.12 ± 0.085	23.8 ± 0.23	3.04 ± 0.086	9.07 ± 0.30	0.180	78.9–145	0.059	0.020
Vandetanib	3.36 ± 0.06	3.52 ± 0.17	2.39 ± 0.034	1.60 ± 0.13	0.102	73.3	0.043	0.064
Cephalexin	2614 ± 0.02	>10,000	2110 ± 0.043	>10,000	69.3	23.9	0.033	N.A.
Ranolazine	88.1 ± 0.043	111 ± 0.092	48.7 ± 0.061	66.3 ± 0.31	1.85	38.5–83	0.038	0.028
Lansoprazole	60.1 ± 0.049	148 ± 0.22	44.0 ± 0.056	66.5 ± 0.24	0.0883	11.8	0.0020	0.0013
Cobicistat	5.29 ± 0.087	12.2 ± 0.11	2.75 ± 0.083	5.27 ± 0.23	0.054	No data	0.020	0.010

$C_{max,u}$, plasma unbound C_{max}; N.A., not applicable.
*IC_{50} values obtained by uptake assay were from Lechner et al. (2016).

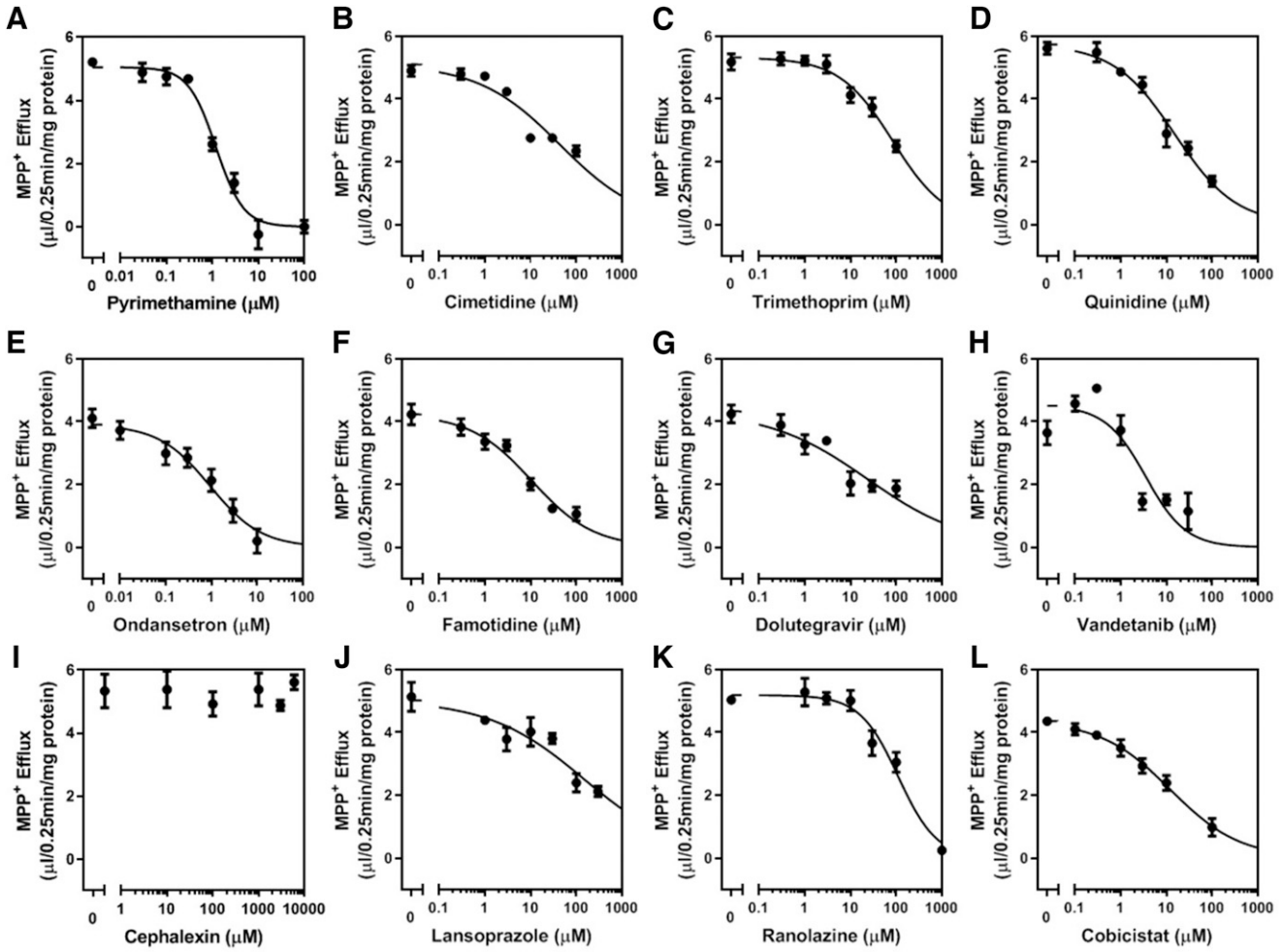

Fig. 2. Inhibitory effect of various compounds on the efflux of [^{3}H]MPP$^+$. Efflux of [^{3}H]MPP$^+$ was determined in the absence and presence of indicated inhibitors in 20 mM NH_4Cl buffer at pH 7.4 for 0.25 minutes. (A) Pyrimethamine, (B) cimetidine, (C) trimethoprim, (D) quinidine, (E) ondansetron, (F) famotidine, (G) dolutegravir, (H) vandetanib, (I) cephalexin, (J) lansoprazole, (K) ranolazine and (L) cobicistat. Each point represents the mean value ± S.E. (n = 3).

When MPP$^+$ was used as a substrate, differences in IC_{50} values between uptake and efflux mode were within 4-fold for 8 out of the 12 inhibitors. For cimetidine, trimethoprim, famotidine, and cephalexin, IC_{50} values were greater in efflux mode, showing 9.9-fold, 10-fold, 6.4-fold, and >3.8-fold differences when compared with the uptake mode, respectively (Fig. 4; Table 1). When metformin was used as a substrate, all IC_{50} values, except for cephalexin, were within 4-fold between uptake and efflux directions (Fig. 4; Table 1).

Discussion

The most commonly used in vitro inhibition assay against MATE1 determines the inhibition potency of extracellularly added compounds by assessing the uptake of probe substrates into MATE1-expressing cells. Thus, this commonly used assay assumes IC_{50} values are identical and independent from whichever direction the substrates are transported. To address whether DDI risk predictions based on regulatory guidelines are different or not depending on the direction of transport, IC_{50} values of various MATE1 inhibitors were generated in "uptake mode" and "efflux mode" based on their extracellular concentrations.

To achieve this, we developed an efflux inhibition assay for MATE1 after preloading two different substrates, MPP$^+$ and metformin, into MATE1-overexpressing cells. Initially, we aimed to measure the amount of substrate being effluxed into the medium. However, because of carryover from the preloading solution and loss of substrate from the cells during necessary subsequent washing steps, efflux clearance was determined based on the time-concentration profiles of remaining substrate within the cells (Fig. 1). The time-dependent decrease in the cells suggested at least two rate constants, one fast and the other much slower, in both substrates, and this phenomenon was more obvious, especially for MPP$^+$. Organic cations are distributed into acidic subcellular compartments such as endosomes (Martínez-Guerrero et al., 2016a), which is referred to as endosomal trapping. According to Martínez-Guerrero, substrate release from endosomes was slow, and the rate constant for initial efflux of MPP$^+$ from MATE1-CHO cells was not changed regardless of the disruption of endosomal trapping by the addition of V-type H^+-ATPase inhibitor. Therefore, assuming that the fast phase represents the efflux from the shallow compartment of the cells, we set 0.25 minutes as a minimum feasible incubation time for further efflux assay. As a preliminary experiment, we examined the dependence of the efflux clearance on the preloaded substrate concentrations (Supplemental Fig. 4). The efflux clearance was decreased, along with an increase in the intracellular concentration, presumably because of the saturation of MATE1-mediated efflux. Apparent K_m values for MPP$^+$ and metformin were estimated in the rage of 10–100 and 100–1000 μM, respectively, which were not largely different from reported K_m values of MATE1-mediated MPP$^+$ and metformin in the uptake direction (47.6 and 208 μM, respectively) (Lechner et al., 2016).

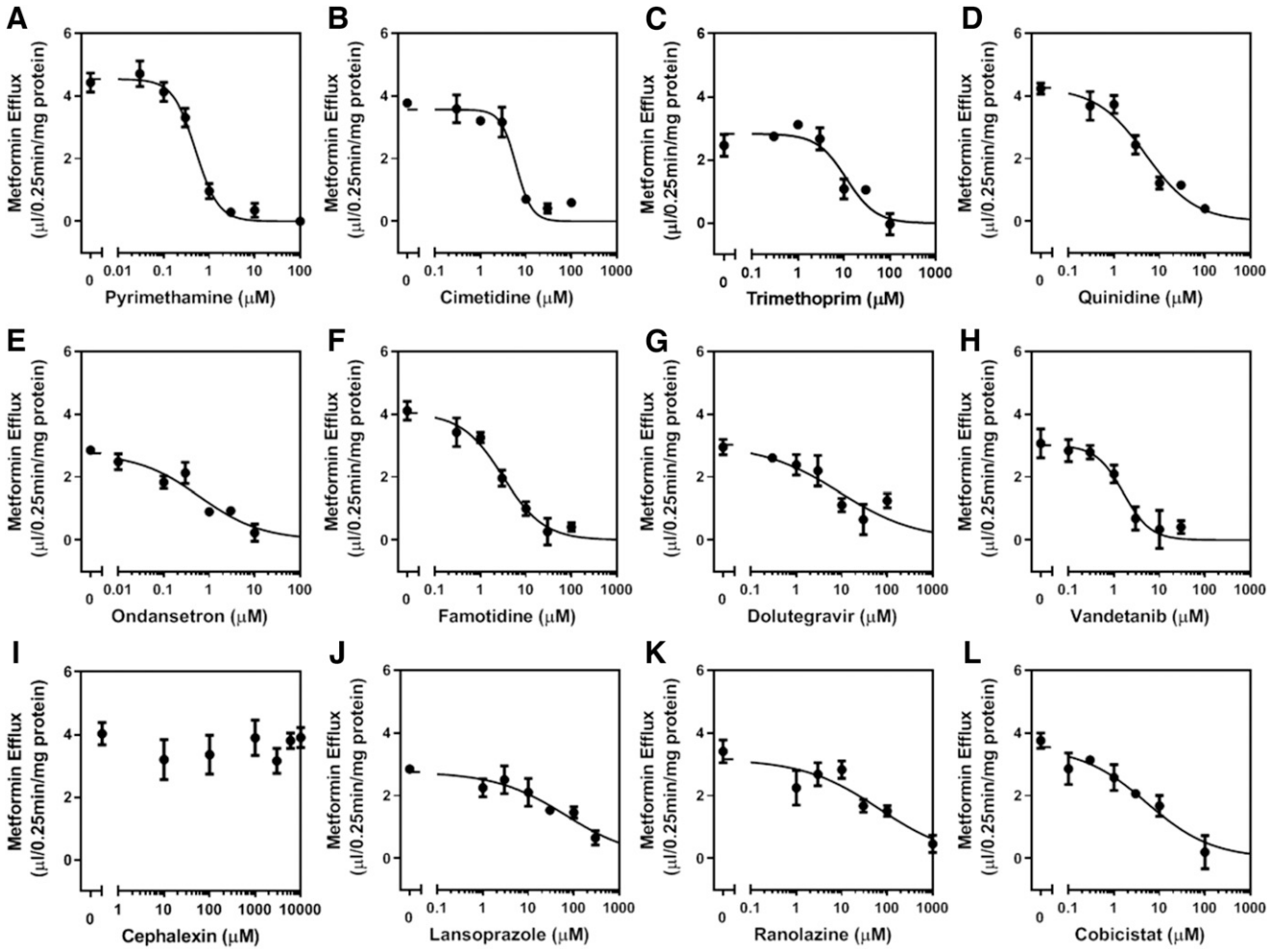

Fig. 3. Inhibitory effect of various compounds on the efflux of [^{3}H]metformin. Efflux of [^{3}H]metformin was determined in the absence and presence of indicated inhibitors in 20 mM NH_4Cl buffer at pH 7.4 for 0.25 minutes. (A) Pyrimethamine, (B) cimetidine, (C) trimethoprim, (D) quinidine, (E) ondansetron, (F) famotidine, (G) dolutegravir, (H) vandetanib, (I) cephalexin, (J) lansoprazole, (K) ranolazine and (L) cobicistat. Each point represents the mean value ± S.E. (n = 3).

Approximation accuracy of these apparent K_m values for the true K_m depends on the intracellular unbound fraction.

This study examined the direction and substrate dependence of IC_{50} values for the MATE1 substrates MPP^+ and metformin by comparing IC_{50} values obtained in uptake and efflux mode (Fig. 4A) and by comparing IC_{50} values between MPP^+ and metformin (Fig. 4B). Regarding direction-dependent inhibition, differences in IC_{50} values for 8 out of 12 compounds were within 4-fold when comparing uptake and efflux mode when MPP^+ was used as the probe substrate, although IC_{50} values for cimetidine, trimethoprim, famotidine, and cephalexin

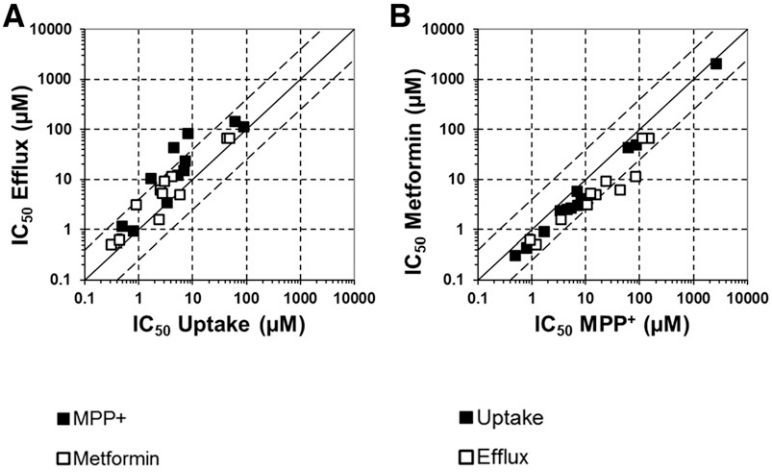

Fig. 4. Comparison of IC_{50} values from the uptake and efflux direction using MPP^+ and metformin as probe substrates. IC_{50} values were determined by nonlinear regression analysis and compared between different transport directions [uptake and efflux (A)] and different substrates [MPP^+ and metformin (B)]. IC_{50} values of cephalexin in the efflux direction were not plotted because there was no observed inhibition at the highest concentration (10 mM). The black line represents the line of unity, and the dotted lines represent 4-fold errors.

differed by greater than 4-fold (Fig. 4A). When metformin was used as the probe substrate, the difference in IC_{50} values between uptake and efflux mode were within 4-fold for every inhibitor tested except cephalexin, which showed very weak inhibition in both assays (Fig. 4A). Regarding substrate dependence, all 12 compounds showed almost identical IC_{50} values (<2.3-fold) for both substrates in uptake assays. Our results are therefore consistent with previously reported substrate-independent IC_{50} values for MPP^+ and metformin (Lechner *et al.*, 2016; Martínez-Guerrero *et al.*, 2016a). On the other hand, IC_{50} values for MPP^+ showed a tendency to be greater than those for metformin in efflux assays. Still, 10 out of the 12 compounds showed differences within 4-fold (Fig. 4B). The mechanism underlying the different substrate dependencies in either the uptake or efflux direction is not yet fully understood. Although this study carefully designed the efflux assays, this study cannot exclude the possibility that inhibitors interact with MATE1 from inside of the cells or by inhibiting the intracellular binding or lysosomal trapping. Since the efflux clearance was calculated using the total concentrations, this parameter theoretically comprises the intrinsic efflux clearance and intracellular unbound fraction. Even during the short incubation time of 0.25 minutes, the inhibitors can distribute to the cells depending on their passive permeability, participate in MATE1 inhibition, and modify the intracellular binding and lysosomal trapping. And this fact therefore indicates difficulties in both efflux and uptake inhibition studies to discriminate MATE1 inhibition from the extracellular space from that from the intracellular space completely as far as the nonpolarized cells are used as host cells. Yet from the viewpoint of preferring a conservative approach to assess DDI to mitigate any risk for patients, we believe that the uptake assay using metformin as the in vitro probe substrate offers the best condition to determine IC_{50} values of investigational drugs as inhibitors of MATE1.

We checked the impact of IC_{50} differences between uptake and efflux direction on predictions of MATE1-mediated clinical DDI risk using IC_{50} values based on metformin as a substrate. The DDI risk assessment according to the most conservative cutoff criteria ($I_{max,u}/IC_{50} > 0.02$) from the latest DDI guidelines from health authorities (Ministry of Health, Labor and Welfare, 2018) provided comparable results between uptake and efflux assays for all compounds. The assessment returned correct predictions of the AUC increase for 9 of the 10 drugs using the $I_{max,u}/IC_{50}$ approach (Table 1), with the only exception being famotidine. The calculated $I_{max,u}/IC_{50}$ values were 1.10 in the uptake direction and 0.322 in the efflux direction for famotidine, which are higher than the regulatory cutoff of 0.02; nevertheless, famotidine instead increased renal clearance of metformin, which was considered a result of modification of other sites by famotidine, such as urine pH modification and inhibition of reabsorption (Hibma et al., 2016). The unbound concentrations of MATE1 inhibitors in the plasma empirically seem to work as surrogates of those inside and/or lumen of the proximal tubules from where the inhibitors can address to MATE1. For instance, the quantitative analysis of dose-dependent effect of pyrimethamine on the renal clearance of metformin yielded apparent IC_{50} values defined from its plasma concentrations comparable with the corresponding in vitro IC_{50} values (Miyake et al., 2020). It remains a challenge to estimate the clinically relevant unbound concentrations of MATE1 inhibitors in the kidney for more precise prediction, particularly when the transporters could concentrate or actively remove inhibitors inside the cells.

Efflux clearances of MPP^+ and metformin were 4- to 6.5-fold smaller compared with uptake clearances (MPP^+: 20 vs. 130, metformin: 14 vs. 55 μl/min per milligram), although the same NH_4Cl concentration (20 mM) was used. Since efflux clearance was based on the total intracellular concentration, different unbound intracellular concentrations might account for the discrepancy. We further speculate that a difference in the delta proton concentration between the outside and the inside of the cells might be one underlying mechanism. Considering that acute exposure to 20 mM NH_4Cl increased intracellular pH to 8.0 when the initial intracellular pH was 7.0 in another experiment (data not shown), the intracellular pH in the efflux assay in which the initial intracellular pH was 7.4 was estimated to be about 8.4, although a pH greater than 8.0 could not be measured because of a limitation of the method. In theory, the proton concentration in the efflux direction is 40 nM in the buffer (pH 7.4) and 4–10 nM within the cells (assuming the intracellular pH is 8.0–8.4), whereas the proton concentration in the uptake direction is 400 nM (pH 6.4) inside the cells and 40 nM in buffer (pH 7.4). Although the relative difference between extracellular and intracellular pH value is about one in both assay conditions, the absolute values of H^+ concentrations, however, differ almost 10-fold. This might affect the duration of initial velocities for uptake and efflux and may have caused an underestimation of efflux clearance under the current conditions.

We compared IC_{50} values of 12 MATE1 inhibitors in both uptake and efflux directions. The IC_{50} values obtained from the uptake assay had a propensity to generate different IC_{50} values from those obtained from the efflux assay as long as metformin was used as the in vitro probe substrate. Moreover, the predictions of clinical inhibition of MATE1 using the $I_{max,u}/IC_{50}$ approach according to the most current regulatory guidance provided accurate predictions of AUC increases for 9 of the 10 inhibitors. The new assay tools, which can evaluate the MATE1 inhibitions separately from outside and from inside the cells, may be expected to produce more physiologically relevant IC_{50} values. From the viewpoint of drug development in pharmaceutical industries, together with our previous study (Lechner et al., 2016), we recommend the uptake assay using metformin as an in vitro probe substrate to determine IC_{50} values of new chemical entities for DDI risk assessment.

Acknowledgments

The excellent technical assistance of Saki Ichimura and Michiru Miyake in performing the in vitro experiments at Nippon Boehringer Ingelheim is gratefully acknowledged. We also thank Dr. Caroline Maclean at Nippon Boehringer Ingelheim and Drs. Mitchell E. Taub and Stephanie Piekos at Boehringer Ingelheim Pharmaceuticals for editing a draft of this manuscript.

Authorship Contributions

Participated in research design: Saito, Ishiguro, Takatani, Bister, Kusuhara.

Conducted experiments: Saito, Takatani.

Performed data analysis: Saito, Takatani, Kusuhara.

Wrote or contributed to the writing of the manuscript: Saito, Ishiguro, Kusuhara.

References

Becker ML, Visser LE, van Schaik RH, Hofman A, Uitterlinden AG, and Stricker BH (2009) Genetic variation in the multidrug and toxin extrusion 1 transporter protein influences the glucose-lowering effect of metformin in patients with diabetes: a preliminary study. *Diabetes* **58**: 745–749.

Chu X, Bleasby K, Chan GH, Nunes I, and Evers R (2016) The complexities of interpreting reversible elevated serum creatinine levels in drug development: does a correlation with inhibition of renal transporters exist? *Drug Metab Dispos* **44**:1498–1509.

Dangprapai Y and Wright SH (2011) Interaction of H^+ with the extracellular and intracellular aspects of hMATE1. *Am J Physiol Renal Physiol* **301**:F520–F528.

European Medicines Agency (2012) EMA guideline on the investigation of drug interactions. 2012. Final CPMP/EWP/560/95.

Gillen CM and Forbush B III (1999) Functional interaction of the K-Cl cotransporter (KCC1) with the Na-K-Cl cotransporter in HEK-293 cells. *Am J Physiol* **276**:C328–C336.

He X, Szewczyk P, Karyakin A, Evin M, Hong WX, Zhang Q, and Chang G (2010) Structure of a cation-bound multidrug and toxic compound extrusion transporter. *Nature* **467**:991–994.

Hibma JE, Zur AA, Castro RA, Wittwer MB, Keizer RJ, Yee SW, Goswami S, Stocker SL, Zhang X, Huang Y, et al. (2016) The effect of famotidine, a MATE1-selective inhibitor, on the pharmacokinetics and pharmacodynamics of metformin. *Clin Pharmacokinet* **55**:711–721.

Ito S, Kusuhara H, Yokochi M, Toyoshima J, Inoue K, Yuasa H, and Sugiyama Y (2012) Competitive inhibition of the luminal efflux by multidrug and toxin extrusions, but not basolateral uptake by organic cation transporter 2, is the likely mechanism underlying the pharmacokinetic drug-drug interactions caused by cimetidine in the kidney. *J Pharmacol Exp Ther* **340**:393–403.

Ivanyuk A, Livio F, Biollaz J, and Buclin T (2017) Renal drug transporters and drug interactions. *Clin Pharmacokinet* **56**:825–892.

Kusuhara H, Ito S, Kumagai Y, Jiang M, Shiroshita T, Moriyama Y, Inoue K, Yuasa H, and Sugiyama Y (2011) Effects of a MATE protein inhibitor, pyrimethamine, on the renal elimination of metformin at oral microdose and at therapeutic dose in healthy subjects. *Clin Pharmacol Ther* **89**:837–844.

Lechner C, Ishiguro N, Fukuhara A, Shimizu H, Ohtsu N, Takatani M, Nishiyama K, Washio I, Yamamura N, and Kusuhara H (2016) Impact of experimental conditions on the evaluation of interactions between multidrug and toxin extrusion proteins and candidate drugs. *Drug Metab Dispos* **44**:1381–1389.

Li Q, Guo D, Dong Z, Zhang W, Zhang L, Huang SM, Polli JE, and Shu Y (2013) Ondansetron can enhance cisplatin-induced nephrotoxicity via inhibition of multiple toxin and extrusion proteins (MATEs). *Toxicol Appl Pharmacol* **273**:100–109.

Lowry OH, Rosebrough NJ, Farr AL, and Randall RJ (1951) Protein measurement with the Folin phenol reagent. *J Biol Chem* **193**:265–275.

Lu M, Radchenko M, Symersky J, Nie R, and Guo Y (2013) Structural insights into H+-coupled multidrug extrusion by a MATE transporter. *Nat Struct Mol Biol* **20**:1310–1317.

Martínez-Guerrero LJ, Evans KK, Dantzler WH, and Wright SH (2016a) The multidrug transporter MATE1 sequesters OCs within an intracellular compartment that has no influence on OC secretion in renal proximal tubules. *Am J Physiol Renal Physiol* **310**:F57–F67.

Martínez-Guerrero LJ, Morales M, Ekins S, and Wright SH (2016b) Lack of influence of substrate on ligand interaction with the human multidrug and toxin extruder, MATE1. *Mol Pharmacol* **90**: 254–264.

Ministry of Health, Labor and Welfare (2018) Guideline on drug interaction for drug development and appropriate provision of information.

Miyake T, Kimoto E, Luo L, Mathialagan S, Horlbogen LM, Ramanathan R, Wood LS, Johnson JG, Le VH, Vourvahis M, et al. (2020) Identification of appropriate endogenous biomarker for risk assessment of multidrug and toxin extrusion protein-mediated drug-drug interactions in healthy volunteers. *Clin Pharmacol Ther* DOI: 10.1002/cpt.2022 [published ahead of print].

Miyauchi H, Moriyama S, Kusakizako T, Kumazaki K, Nakane T, Yamashita K, Hirata K, Dohmae N, Nishizawa T, Ito K, et al. (2017) Structural basis for xenobiotic extrusion by eukaryotic MATE transporter. *Nat Commun* **8**:1633.

Motohashi H and Inui K (2013) Multidrug and toxin extrusion family SLC47: physiological, pharmacokinetic and toxicokinetic importance of MATE1 and MATE2-K. *Mol Aspects Med* **34**: 661–668.

Nakada T, Kudo T, Kume T, Kusuhara H, and Ito K (2019) Estimation of changes in serum creatinine and creatinine clearance caused by renal transporter inhibition in healthy subjects. *Drug Metab Pharmacokinet* **34**:233–238.

Prasad B, Johnson K, Billington S, Lee C, Chung GW, Brown CD, Kelly EJ, Himmelfarb J, and Unadkat JD (2016) Abundance of drug transporters in the human kidney cortex as quantified by quantitative targeted proteomics. *Drug Metab Dispos* **44**:1920–1924.

Stocker SL, Morrissey KM, Yee SW, Castro RA, Xu L, Dahlin A, Ramirez AH, Roden DM, Wilke RA, McCarty CA, et al. (2013) The effect of novel promoter variants in MATE1 and MATE2 on the pharmacokinetics and pharmacodynamics of metformin. *Clin Pharmacol Ther* **93**:186–194.

Tanaka Y, Hipolito CJ, Maturana AD, Ito K, Kuroda T, Higuchi T, Katoh T, Kato HE, Hattori M, Kumazaki K, et al. (2013) Structural basis for the drug extrusion mechanism by a MATE multidrug transporter. *Nature* **496**:247–251.

Terada T and Inui K (2008) Physiological and pharmacokinetic roles of H+/organic cation antiporters (MATE/SLC47A). *Biochem Pharmacol* **75**:1689–1696.

Thomas JA, Buchsbaum RN, Zimniak A, and Racker E (1979) Intracellular pH measurements in Ehrlich ascites tumor cells utilizing spectroscopic probes generated in situ. *Biochemistry* **18**:2210–2218.

Tsuda M, Terada T, Ueba M, Sato T, Masuda S, Katsura T, and Inui K (2009) Involvement of human multidrug and toxin extrusion 1 in the drug interaction between cimetidine and metformin in renal epithelial cells. *J Pharmacol Exp Ther* **329**:185–191.

U.S. Food and Drug Administration (2020) In vitro drug interaction studies-cytochrome P450 enzyme- and transporter-mediated drug interactions.

Yonezawa A and Inui K (2011a) Importance of the multidrug and toxin extrusion MATE/SLC47A family to pharmacokinetics, pharmacodynamics/toxicodynamics and pharmacogenomics. *Br J Pharmacol* **164**:1817–1825.

Yonezawa A and Inui K (2011b) Organic cation transporter OCT/SLC22A and H(+)/organic cation antiporter MATE/SLC47A are key molecules for nephrotoxicity of platinum agents. *Biochem Pharmacol* **81**:563–568.

Address correspondence to: Hiroyuki Kusuhara, Laboratory of Molecular Pharmaceutics, Graduate School of Pharmaceutical Sciences, The University of Tokyo, 7-3-1, Hongo, Bunkyo-ku, Tokyo 113-0033, Japan. E-mail: kusuhara@mol.f.u-tokyo.ac.jp